

DRY-OUT CHF CHARACTERISTICS OF R134a FLOW BOILING IN A HORIZONTAL
 HELICALLY-COILED TUBE

Chang-Nian Chen, Ji-Tian Han, Li Shao
 School of Energy and Power Engineering,
 Shandong University
 Jinan, Shandong, 250061, P.R. China
 jthan@sdu.edu.cn

Tien-Chien Jen
 Department of Mechanical Engineering,
 University of Wisconsin-Milwaukee
 Milwaukee, WI, 53201, USA
 jent@uwm.edu

ABSTRACT

An experimental study was carried out to investigate the dry-out critical heat flux (CHF) characteristics of R134a flow boiling in a horizontal helically-coiled tube. The test section was heated uniformly by DC high-power sources and the geometrical parameters are the outer diameter of 10 mm, inner diameter of 8.4 mm, coil diameter of 300 mm, helical pitch of 75 mm and valid heated length of 1.89 m. The experimental conditions are the outlet pressures of 0.30-0.95 MPa, mass fluxes of 60-500 kg/m²s, inlet qualities of -0.36-0.35 and heat fluxes of 7-50 kW/m². In total of sixty-eight 0.2 mm T-type thermocouples were set along the tube to measure wall temperatures exactly. A method based on the event-driven Agilent BenchLink Data Logger Pro software was developed to determine the occurrence of CHF. It was found that the wall temperatures jumped abruptly once the CHF occurred. The CHF usually starts to form at the front and offside (270° and 90°) of the sections near outlet. The CHF value increases largely with increasing mass flux and decreases slightly with increasing pressure. It decreases nearly linearly with increasing inlet qualities, while it decreases acutely with increasing critical qualities under larger mass flux conditions. An experimental correlation was developed to estimate dry-out CHF of R134a flow boiling in horizontal helically-coiled tubes under current conditions compared with the calculated results of Bowring and Shah correlations.

Key words: dry-out CHF; horizontal helically-coiled tubes; boiling heat transfer; R134a

NOMENCLATURE

A heated area of the test section (m^2)
 A' coefficient in Eq.(9)
 B_o boiling number, $B_o = \frac{q_{cr}}{G \cdot \gamma}$

C' coefficient in Eq.(9)
 C_p thermal capacity ($kJ \cdot kg^{-1} K^{-1}$)
 D hydraulic diameter (m)
 D_c coil diameter (m)
 D_n Dean number, $D_n = Re \cdot \left(\frac{d_i}{D_c}\right)^{0.5}$
 G mass flux ($kgm^{-2}s^{-1}$)
 I current (A)
 L valid heated length (m)
 N_d liquid-gas density ratio, $N_d = \frac{\rho_l}{\rho_g}$
 P_A power value logged by Agilent software (kW)
 Pe Peclet number, $Pe = Re \cdot Pr$
 P_e power supplies for test section (kW)
 P_p power supplies for preheated section (kW)
 p pressure (MPa)
 Pr Prandtl number, $Pr = \frac{C_p \cdot \mu}{k}$
 Re Reynolds number, $Re = \frac{GD}{\mu}$
 S section symbol of the test tube
 T_0 temperature rise of an empty tube as same as the test section with increasing heat flux \dot{q} (K)
 T_i temperature at time i ($^{\circ}C$)
 T_{i-1} temperature at time $i-1$ ($^{\circ}C$)
 U voltage (V)
 q_{cr} average critical heat flux (kWm^{-2})

q_{cr1}	critical heat flux calculated by Agilent software (kWm^{-2})
q_{cr2}	critical heat flux logged in DC power supplies (kWm^{-2})
r_i	inner radius of the test tube (m)
r_o	outer radius of the test tube (m)
x_{cr}	critical quality
x_i	inlet quality
x_o	outlet quality
δT	temperature difference value defined according to the experimental conditions (K)
Δh_i	inlet subcooling enthalpy ($J \cdot kg^{-1}$)
δq	increment of heat flux (kWm^{-2})
δ	error of T-type thermocouples (K)
<i>Greek symbols</i>	
γ	latent heat of evaporation ($J \cdot kg^{-1}$)
ρ	density (kgm^{-3})
μ	dynamic viscosity (Pas)
<i>Subscripts</i>	
exp	experimental data
g	gas phase
l	liquid phase
pre	prediction data
ss	stainless steel

INTRODUCTION

Critical heat flux (CHF) is one of the most significantly monitored parameters for operating heating equipment such as refrigeration evaporator, once-through boiler water-wall and nuclear reactor bundles, etc. Under the uniformly heating conditions, the heat transfer coefficient decreases suddenly and the heated wall temperature increases abruptly when the CHF occurs [1]. Without effective control, the wall temperature will exceed the maximum allowable temperature of materials, damaging the heating facilities and possibly endangering those who operate the equipment. Because of the importance of CHF to engineering applications, thousands of researchers have developed more than a thousand correlations and hundreds of methods for estimating CHF in the past four decades, including theory analysis and experimental investigations [2-11]. Although successful methods such as fluid to fluid modeling [2], look-up table (LUT) [3] and neural network forecasting [4] are widely used, there has not been one revealing the essence of CHF due to its complicated mechanism, especially in complex flow channels and various conditions. However, for some particular situations, experimental study of CHF from which adequate accurate results can be obtained is utilizable.

Based on different theoretical explanations for the trigger mechanism of CHF in different conditions, CHF is generally classified into two types named DNB (departure from nucleate boiling) CHF and dry-out CHF, respectively. The former, which is more suited toward nuclear reactors, usually occurs under much higher heat flux than the later. For general industry processes dry-out CHF is more frequently used and often results in accidents. Therefore, studying the characteristics of dry-out CHF is a necessary to ensure the safety of the process.

More work has been done with CHF in straight tubes with various fluids. Bowring [5] proposed an accurate correlation for dry-out heat flux in round tube using water as working fluid over the pressure range 0.7-12 MPa. His correlation was developed based on 3800 experimental data and had an error of 7% for CHF in water. Katto and Ohno [6] investigated on CHF of forced convective boiling in uniformly heated vertical tubes. Their experiments covered nearly all the main characteristic regimes of CHF, but concerned only about vertical tubes. Shah [7] improved one general correlation for upflow CHF in vertical tubes comparing with Bowring and Katto correlations. His new correlation greatly agreed with CHF data of 23 fluids from 62 independent sources. Therefore, it was one of the most extensively used CHF correlations. Wong et al. [8] devised a new forecasting method for horizontal straight tubes. They established the models for the prediction of CHF in horizontal forced-convective flow from CHF in vertical flow using correction factors. The results gave a satisfying agreement with data. Kim et al. [9] conducted CHF experiments of water in vertical tubes under low pressure and low flow conditions (LPLF). They compared parametric trends under these special conditions with previous general understandings, considering the complex effects of system pressure and tube diameter. Pioro et al. [10] compared the R134a CHF data in vertical tubes with the water CHF look-up table and indicated the noticeable points for limiting critical quality range and low mass flux. Groeneveld et al. [3] updated the CHF look-up table, which was a normalized data bank for vertical 8 mm water-cooled tube based on more than 30,000 data points; Sindhuja et al. [11] studied mixture R407c CHF characteristics in upflow vertical tubes and compared the results with pure fluids. In addition, some efforts were contributed to investigate the CHF in nuclear reactor bundles [12-16].

For helically-coiled tubes, heat transfer and pressure drop characteristics of flow boiling have been widely studied [17-21]. A few of researchers investigated the CHF characteristics in helical coils. Jensen and Bergles [22-23] performed a series of experimental studies on boiling heat transfer and CHF characteristics in helical coils using R113 as working fluid. They mainly emphasized on the effect of an outside heat flux tilt on the CHF and found that subcooled CHF was degraded in coils relative to straight tubes, and the degradation increased with increasing the tube diameter-to-coil diameter ratio and the mass velocity, while dry-out CHF was enhanced and increased with increasing the tube diameter-to-coil diameter ratio. CHF initially increased with increasing mass velocity but began to

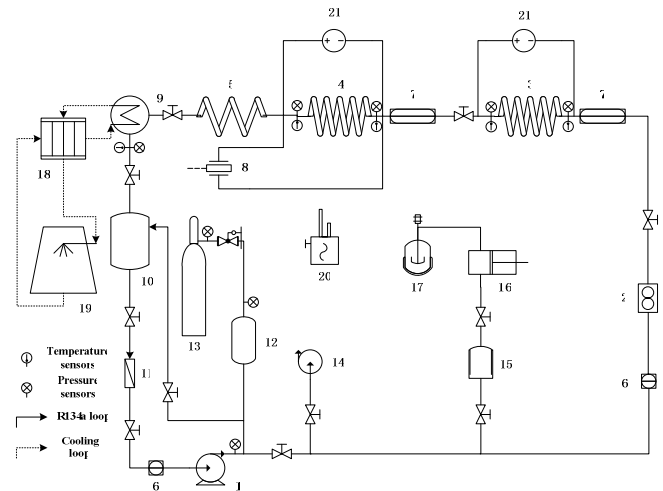
decrease after a maximum value. Styrikovich et al. [24] presented their investigation on the temperature regime of a helical coil with both upflow and downflow of a steam-water mixture. They found that CHF in coils was higher than in a vertical straight tube, while the temperature regime of the coil tube in the post-dryout region was less severe. Jayanti and Berthoud [25] conducted an experiment about high-quality dryout in helical coils. They analyzed the influence of pressure, coil diameter, mass flux and heat flux on CHF and firstly proposed the correlations for the related area. Ma et al. [26] also carried out a research on high-quality CHF characteristics in helically coiled tubes. They evaluated the “local condition hypothesis” based on experimental data and discussed the “film inversion” phenomenon in coils. Zhang et al. [27] studied the deterioration of vapor-water boiling heat transfer in a helically-coiled tube and collected 272 data points for look-up table. However, their database was based on a helically-coiled tube set vertically, which can not cover horizontal ones.

In summary, previous studies were mainly related to CHF behaviors in straight tubes, or bundles concerned by nuclear reactor only, using water which required high pressure and temperature or some CFCs substance which is toxic to environment. Investigations on CHF in helically-coiled tubes are scarce. As a kind of heat transfer enhancement tube, the helically-coiled tube has been widely used in energy engineering and petrochemical industry [18,21]. Compared to straight tube, it has merits of high heat transfer efficiency and compact structure. It has a greater heat transfer area than a straight tube in the same amount of space. This is especially true for applications in aircrafts and submarines, which both need narrow space to operate and the tube should be placed horizontally with a lower gravity center. Because of the special structure, characteristics of CHF in this kind of tube are different from straight one, which should be studied. Considering the high latent heat of evaporation of water and the destruction of the ozone layer by CFCs, experiments for studying CHF characteristics in a helically-coiled tube were performed using R134a as working fluid in this paper. The axis of the helically-coil is horizontal, as shown in Fig.1.

EXPERIMENTAL APPARATUS AND PROCEDURE

Experimental Circle Loop

The experimental set-up consists of two circle loops, the working loop (R134a) and the cooling loop (30% CaCl₂ solution), as shown in Fig.1. It includes the following components: canned motor pump, coriolis mass flowmeter, preheated/test sections, precision DC power supplies, condenser, refrigeration chilling unit, N₂-gas accumulator and data acquisition system. The working loop is designed for pressure of 1.6 MPa and temperature of 200 °C, preheated section power of 24 V × 300 A and test section of 60 V × 500 A. The refrigeration chilling unit has a maximum output of 50 kW.



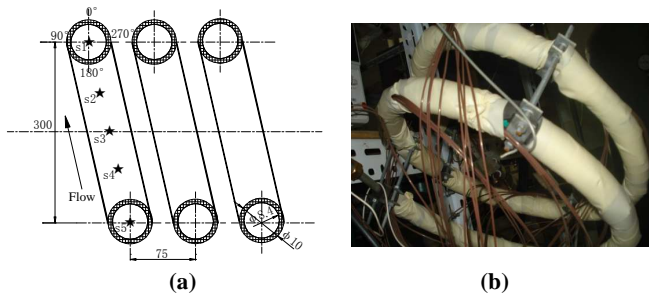
1 canned motor pump, **2** coriolis mass flowmeter, **3** preheated section, **4** test section, **5** flow pattern observing section, **6** sight glass, **7** visual section, **8** differential pressure gage, **9** condenser, **10** receiver tank, **11** dry-strainer, **12** accumulator, **13** N₂ gas tank, **14** vacuum pump, **15** buffer tank, **16** refrigerant pump, **17** refrigerant tank, **18** chilling unit, **19** cooling tower, **20** halogens leak detector, **21** DC power supply

FIG.1 SCHEMATIC DIAGRAM OF THE EXPERIMENTAL CIRCLE LOOP

Test Section and Installation

The test section is made of stainless steel tube (SUS304), as shown in Fig.2. It has a 300 mm coil diameter and a 75 mm helical pitch and its outer diameter and inner diameter are 10 mm and 8.4 mm, respectively. The valid heated coiled length is 1.89 m. The test section is directly electrified by high current DC power supplies to generate constant heat flux (ignoring resistance variation).

The temperatures of the working fluid R134a at the inlet and outlet of the test section are measured with 0.3 mm T-type sheathed thermocouples (copper-constantan). The precision pressure sensors are set at the same positions as thermocouples in order to measure the inlet and outlet pressures accurately. The temperatures of outside wall are measured by 68 0.2 mm T-type thermocouples set along the test tube. Eight symmetrical positions of each coil of the helically-coiled tube, i.e., every quarter-coil, as S1-S5 indicated in Fig.2(a), are selected for the measuring sections where four thermocouples are set evenly around the circumferences, 0°, 90°, 180° and 270° as indicated in Fig.2(a). The four positions of the same section (0°-270°) are named upside, offside, underside and frontside, respectively. The inlet section and the outlet section are both 5 mm away from the copper electrodes connected with DC power supplies. Three pairs of clamps are installed to stop from distortion of test tube, as indicated in Fig.2(b). All the experimental signals are collected and processed by Agilent 34980A data acquisition system.



(a) schematic diagram of the test tube structure
(b) photograph of the test section with attenuator

FIG.2 STRUCTURE DIAGRAM OF THE TEST SECTION

Experimental Conditions and Procedure

The CHF experiments were carried out at outlet pressures of 0.30-0.95 MPa, mass fluxes of 60-500 kg/m²s, inlet qualities of -0.36-0.35, and heat fluxes of 7-50 kW/m².

The procedures were conducted as follows. The helically-coiled tube was placed horizontally and connected to the system with flange insulated. Before each single experiment heat balance testing was performed and results showed that the heat losses were no more than 5%. R134a from the receiver tank is circulated through the whole system by canned motor pump. The mass flux can be controlled by adjusting the speed of motor and control valves. The pressure is controlled by adjusting mass flux of cooling loop, power supply of preheated section and N₂-gas accumulator. When the pressure and mass flux of the system are stabilized to predetermined values, the inlet temperature is controlled by increasing or decreasing power supply to preheated section. The power supply to test section is increased rapidly at the beginning, and then slowly at each step of about 0.05 kW/m² until CHF occurs. A method based on the event-driven Agilent BenchLink Data Logger Pro software was developed to determine the occurrence of CHF. Critical heat flux phenomena are considered to occur once any wall temperature T_i detected by thermocouples satisfies Eq.(1) and Eq.(2). Subsequently, the Agilent software sends signal to cut off power supply within 0.1 second.

$$T_0 - (T_i - T_{i-1}) \leq \delta T + \delta t \quad (1)$$

$$T_0 = \frac{2 \cdot \delta q \cdot r_i}{(r_o^2 - r_i^2) \cdot \rho_{ss} \cdot C_{p,ss}} \quad (2)$$

Experimental uncertainties

The directly measured parameters in experiments include length, temperature, pressure, mass flux, voltage and current. Based on the instructions of experimental equipments and verified data sheet, the maximum uncertainty in measuring

length and inner diameter of test section is $\pm 0.014\%$ and $\pm 0.27\%$, respectively; the maximum uncertainty in measuring temperature is $\pm 0.9\%$; the maximum uncertainty in measuring pressure is $\pm 1\%$; the maximum uncertainty in measuring mass flux is $\pm 2.4\%$; the maximum uncertainty in measuring voltage and current is $\pm 0.68\%$ and $\pm 2\%$, respectively. Thus, the maximum uncertainty in measuring the heated area of test tube and critical heat flux value is about $\pm 0.27\%$ and $\pm 2.1\%$, respectively, according to Moffat's experimental error transfer procedure [28].

EXPERIMENTAL RESULTS AND DISCUSSION

Data Reduction

In order to introduce the characteristics of CHF in horizontal helically-coiled tube in experiments, critical heat flux q_{cr} (CHF value), inlet vapor quality x_i , outlet vapor quality x_o and critical vapor quality x_{cr} are needed. They are calculated as follows.

Ignoring the resistance variation of the test tube, the average critical heat flux q_{cr} is calculated according to Eq.(3)-Eq.(6).

$$q_{cr} = \frac{q_{cr1} + q_{cr2}}{2} \quad (3)$$

$$q_{cr1} = \frac{P_A}{A} \quad (4)$$

$$q_{cr2} = \frac{U \cdot I}{A} \quad (5)$$

$$A = 2\pi r_i L \quad (6)$$

Considering the heat losses of system within 5%, vapor qualities x_i , and x_o are evaluated by Eq.(7) and Eq.(8) based on heat balance.

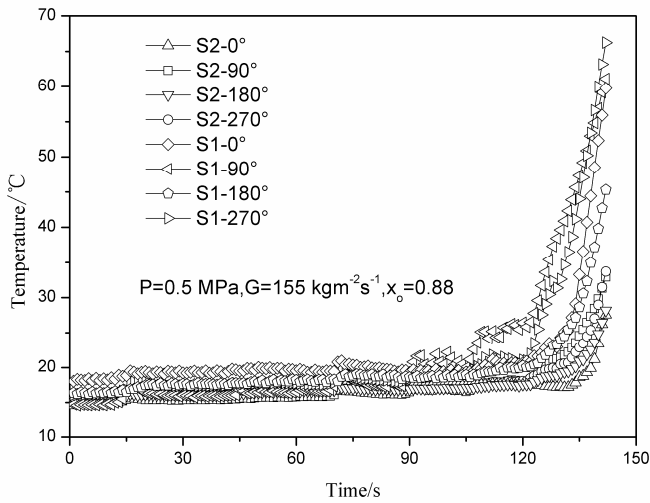
$$x_i = \frac{0.95 P_p}{\pi \cdot G \cdot r_i^2 \cdot \gamma} - \frac{\Delta h_i}{\gamma} \quad (7)$$

$$x_o = x_i + \frac{0.95 P_e}{\pi \cdot G \cdot r_i^2 \cdot \gamma} \quad (8)$$

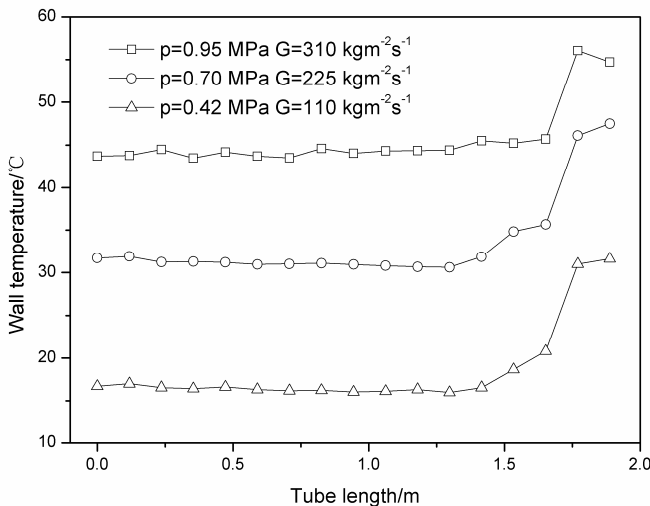
Strictly speaking, when dry-out CHF happened, outlet of the test section has high vapor quality and the thermodynamic equilibrium break [29]. However, calculating the real critical vapor quality is difficult. For the purpose of evaluating CHF, it is feasible to suppose the critical vapor quality x_{cr} equals the thermodynamic equilibrium outlet vapor quality x_o .

Characteristics of Wall Temperature Distribution

Dry-out CHF usually starts at the outlet section near outlet copper electrode and spreads to the whole section circumference immediately; the wall temperature will then increase very quickly. For example, at pressure of 0.50 MPa and mass flux of 155 kg/m²s the rise of temperatures of the two sections S1 and S2 at the end of test tube are shown in Fig.3(a). They vary almost from 15 °C to 70 °C rapidly. And wall temperatures of S1 rise much earlier than those of S2. And the wall temperatures at the front and offside (270° and 90°) frequently are much higher than the other two sides. This refers to the “film inversion” phenomenon in helical coils as reported by Hewitt and Jayanti [30] and Ma et al. [26]. When dry-out CHF occurs, the thinner liquid films at the front and offside can be easily torn out under high vapor quality conditions.



(a)

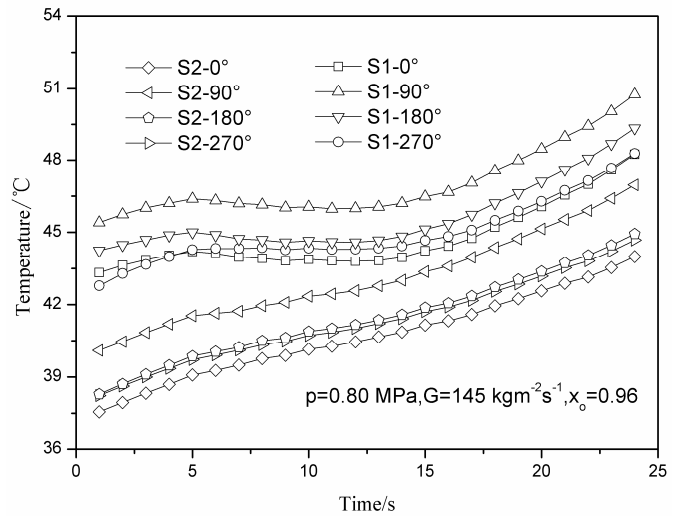


(b)

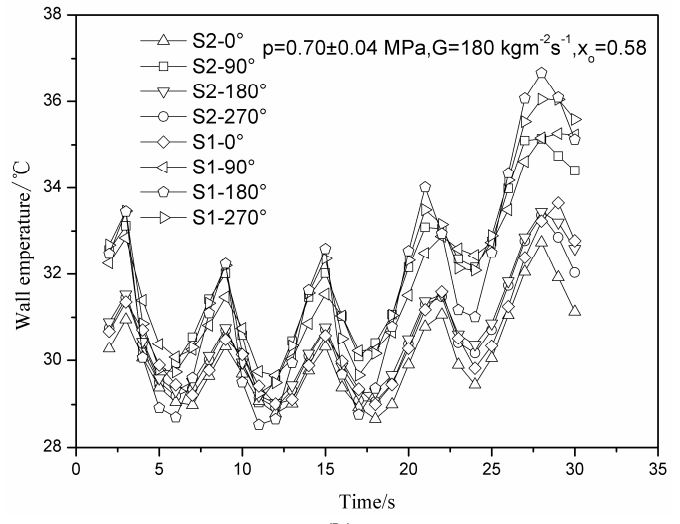
FIG.3 CHARACTERISTICS OF WALL TEMPERATURE DISTRIBUTION IN OUTER SECTIONS AND ALONG THE TEST TUBE

The location of the sudden temperature rise of sections along the heated length is shown in Fig.3(b). Under three different experimental conditions, the wall temperatures show the same abrupt rise regularly along the heated length of test tube.

After the CHF occurs, all the wall temperatures sometimes will rise slowly even decrease to some extent, as shown in Fig.4(a), when there is a high outlet vapor quality. This refers to the steady dry-out area in which the heating facilities may not be destroyed immediately. On the contrary, when the outlet vapor quality is lower, the wall temperatures will show a fluctuating state with pressure wave, as shown in Fig.4(b). This is caused by intermittent rewetting of liquid phase remained in helically-coiled tube, which is synchronously affected by both gravity and centrifugal force.



(a)

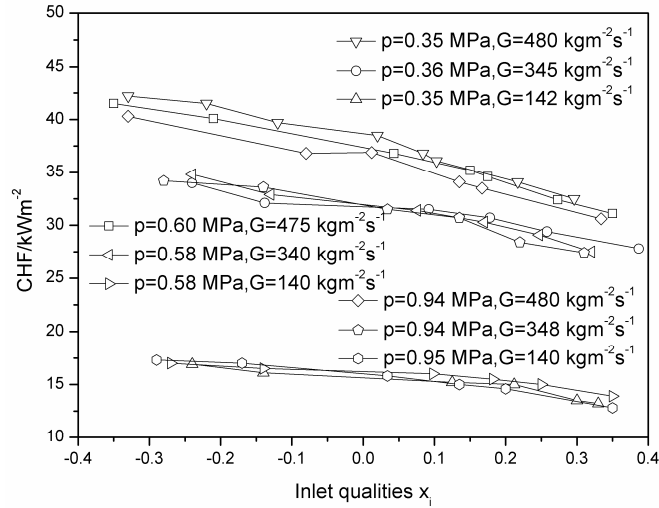


(b)

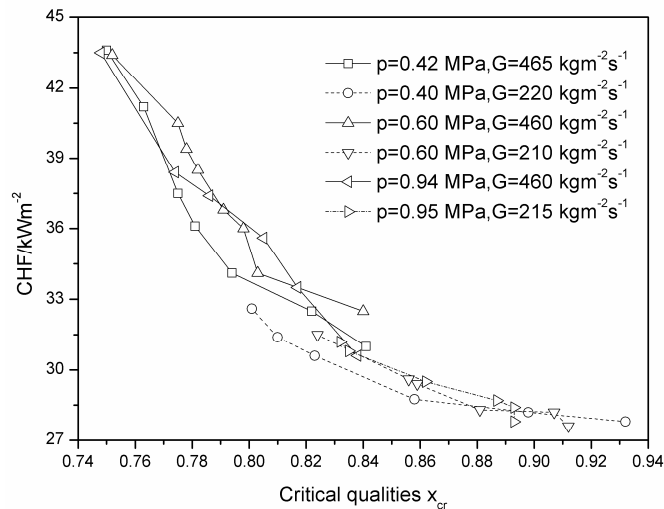
FIG.4 CHARACTERISTICS OF CIRCUMFERENCE WALL TEMPERATURE IN DIFFERENT OUTLET VAPOR QUALITIES

Effect of System Parameters on CHF

The effect of system parameters including inlet vapor quality, outlet pressure, mass flux and critical vapor quality, are shown in Fig.5.



(a)



(b)

FIG.5 EFFECT OF INLET QUALITIES AND CRITICAL QUALITIES ON DRY-OUT CHF

Figure 5(a) shows that CHF values have an approximately linear declining trend with increasing inlet vapor qualities, especially at high mass flux, and the regularity maintains at different pressures and mass fluxes. Outlet pressures do not seem to affect the CHF, and it seems like that CHF values decrease a little with increasing pressures at the same inlet vapor qualities and mass fluxes. While mass fluxes have more effect on CHF, and CHF values increase much more with

increasing mass fluxes at the same inlet vapor qualities and outlet pressures.

Figure 5(b) shows that CHF values decrease with increasing critical vapor qualities. The critical vapor qualities at higher mass fluxes are lower than those at lower mass fluxes. However, critical vapor qualities have a more obvious effect on CHF at higher mass fluxes, which is reflected in Fig.5(b) based on the fact that generally the slopes of real lines (representing higher mass fluxes) are bigger than those of broken lines (representing lower mass fluxes).

Comparison with Classical Correlations

Among existing correlations for CHF, Bowring [5] and Shah [7] correlations are more verified and convenient to use. Bowring correlation is expressed as follows:

$$q_{cr} = \frac{A' + 0.25D \cdot G \cdot \Delta h_i}{C' + L} \quad (9)$$

This correlation was derived from the following parameter ranges: $p \in (0.2, 19)$ MPa, $D \in (2, 45)$ mm, $L \in (150, 3700)$ mm and $G \in (136, 18600)$ kg/m²s. Shah correlation is expressed as follows:

$$B_o = f\left(\frac{L}{D}, Pe \cdot Fr^{0.4} \cdot \left(\frac{\mu_l}{\mu_g}\right)^{0.6}, x_i\right) \quad (10)$$

This correlation was applied widely for the parameter ranges with a mean error of 16%: reduced pressures of 0.0014-0.96 MPa, $L/D \in (1.3, 940)$, $D \in (0.315, 37.5)$ mm, and $G \in (3.9, 29051)$ kg/m²s.

To evaluate the validity of Bowring and Shah correlations for CHF in helically-coiled tubes, experimental data were compared with the calculated results at the same conditions, as shown in Fig.6. It shows that the calculated values from the two correlations are both smaller than experiment results, with average errors of 40% and 35%, respectively. Actually, both of them can accurately predict CHF in straight tube, but are not suitable for R134a CHF in horizontal helically-coiled tubes under current experimental conditions.

A new correlation for current experimental conditions is developed as follows with an error of $\pm 15\%$, as shown in Fig.6.

$$B_o = 1.135 \times 10^{-7} Re^{2.32} D_n^{-2.5} N_d^{0.19} x_i^{-0.58} \quad (11)$$

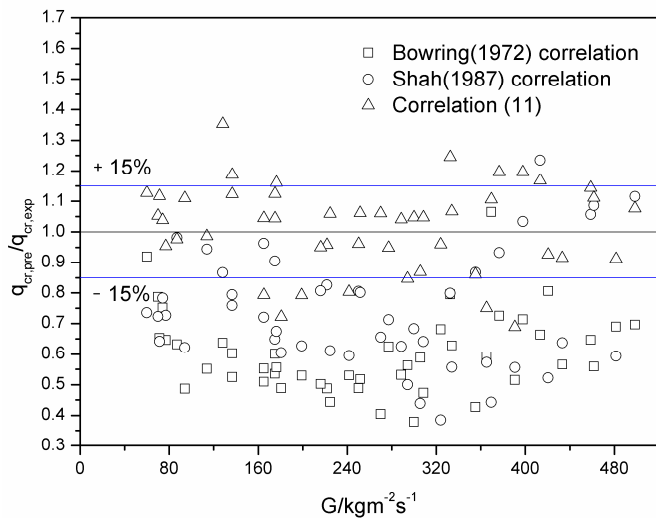


FIG.6 COMPARISON OF EXPERIMENTAL DATA WITH CLASSICAL CORRELATIONS

CONCLUSIONS

Experiments for dry-out CHF in horizontal helically-coiled tube have been conducted using alternative refrigerant R134a. From the analysis of wall temperature distribution and effect of system parameters, conclusions can be drawn as follows.

(1) Dry-out CHF usually occurs at outlet sections near the end of the test tube, and it spreads to the whole section circumference immediately. The wall temperatures at the front and offside (270° and 90°) frequently are higher than the other two sides.

(2) When there is a high outlet vapor quality after the CHF occurs, all the wall temperatures in the steady dry-out area will sometimes rise smoothly or even decrease to some extent. On the contrary, when the outlet vapor quality is lower the wall temperatures will show a fluctuant state with pressure wave, which is caused by intermittent rewetting of liquid-phase remaining in helically-coiled tube as described in text.

(3) CHF values have an approximately linear decline trend with increasing inlet vapor qualities, and decrease with increasing critical vapor qualities, especially at high mass flux. At the present range of experimental conditions, mass fluxes have the most effect on CHF, while pressures have the least.

(4) Compared to experimental data, both of Bowring and Shah correlations are invalid for evaluating CHF in horizontal helically-coiled tubes. A new correlation for current experimental conditions is developed with an error of $\pm 15\%$.

ACKNOWLEDGMENTS

This work was supported by The National Natural Science Foundation of China (No.50776055) and The Natural Science Foundation of Shandong Province, China (No.Y2007F10). Dr. Tien-Chien Jen would also like to acknowledge partial financial support from EPA (USA) award RD 833357.

REFERENCES

- [1] Collier, J.G., and Thome, J.R., 1994, *Convective Boiling and Condensation*, 3rd edition, Clarendon Press, Oxford, England, pp. 329-365.
- [2] Ahmad, S.Y., 1973, "Fluid to Fluid Modeling of Critical Heat Flux: A Compensated Distortion Model," *International Journal of Heat and Mass Transfer*, **16**(3), pp. 641-662.
- [3] Groeneveld, D.C., Shan, J.Q., and Vasic, A.Z., et al, 2007, "The 2006 CHF Look-up Table," *Nuclear Engineering and Design*, **273**(15-17), pp. 1909-1922.
- [4] Vaziri, N., Hojabri, A., and Erfani, A., et al, 2007, "Critical Heat Flux Prediction by Using Radial Basis Function and Multilayer Perceptron Neural Networks: A Comparison Study," *Nuclear Engineering and Design*, **237**(4), pp. 377-385.
- [5] Bowring, R.W., 1972, "A Simple But Accurate Round Tube Uniform Heat Flux, Dry-out Correlation Over the Pressure Range, 0.7-12 MN/m² (100-2500 psia)," Br. Report, AEEW-R789, Winfrith, U.K..
- [6] Katto, Y., and Ohno, H., 1984, "An Improved Version of the Generalized Correlation of Critical Heat Flux for the Forced Convective Boiling in Uniformly Heated Vertical Tubes," *International Journal of Heat and Mass Transfer*, **27**(9), pp. 1641-1648.
- [7] Shah, M.M., 1987, "Improved General Correlation for Critical Heat Flux During Upflow in Uniformly Heated Vertical Tubes," *International Journal of Heat and Fluid Flow*, **8**(4), pp. 325-335.
- [8] Wong, Y.L., Groeneveld, D.C., and Cheng, S.C., 1990, "CHF Prediction for Horizontal Tubes," *International Journal of Multiphase Flow*, **16**(1), pp. 123-138.
- [9] Kim, H.C., Bark, W.P., and Chang, S.H., 2000, "Critical Heat Flux of Water in Vertical Round Tubes at Low Pressure and Low Flow Conditions," *Nuclear Engineering and Design*, **199**(1-2), pp. 49-73.
- [10] Piro, I.L., Groeneveld, D.C., and Cheng, S.C., et al, 2001, "Comparison of CHF Measurements in R-134a Cooled Tubes and the Water CHF Look-up Table," *International Journal of Heat and Mass Transfer*, **44**(1), pp. 73-88.
- [11] Sindhuja, R., Balakrishnan, A.R., and Murthy, S.S., 2008, "Critical Heat Flux of R-407c in Upflow Boiling in a Vertical Pipe," *Applied Thermal Engineering*, **28**(8-9), pp. 1058-1065.
- [12] Hwang, D.H., Baek, W.P., and Chang, S.H., 1993, "Development of a Bundle Correction Method and Its Application to Predicting CHF in Rod Bundles," *Nuclear Engineering and Design*, **139**(2), pp. 205-220.
- [13] Cheng, X., and Müller, U., 1998, "Critical Heat Flux and Turbulent Mixing in Hexagonal Tight Rod Bundles," *International Journal of Multiphase Flow*, **24**(8), pp. 1245-1263.
- [14] Piro, I.L., Cheng, S.C., and Vasic, A.Z., et al, 2000, "Some Problems for Bundle CHF Prediction Based on CHF Measurements in Simple Flow Geometries," *Nuclear Engineering and Design*, **201**(2-3), pp. 189-207.

- [15] Chen, J., Liao, J.R., and Kuang, B., et al, 2004, "Fluid-to-fluid Modeling of Critical Heat Flux in 4×4 Rod Bundles," *Nuclear Engineering and Design*, **232**(1), pp. 47-55.
- [16] Kolev, N.I., 2007, "Check of the 2005 Look-up Table for Prediction of CHF in Bundles," *Nuclear Engineering and Design*, **237**(9), pp. 978-981.
- [17] Xin R.C., Awwad A., Dong Z.F., et al, 1997, "An Experimental Study of Single-phase and Two-phase Flow Pressure Drop in Annular Helicoidal Pipes," *International Journal of Heat and Mass Transfer*, **18**(5), pp. 482-488.
- [18] Han, J.T., Lin, C.X., and Ebadian, M.A., 2005, "Condensation Heat Transfer and Pressure Drop Characteristics of R-134a in an Annular Helical Pipe," *International Communications in Heat and Mass Transfer*, **32**(10), pp. 1307-1316.
- [19] Wongwises, S., and Polsongkram, M., 2006, "Evaporation Heat Transfer and Pressure Drop of HFC-134a in a Helically Coiled Concentric Tube-in-tube Heat Exchanger," *International Journal of Heat and Mass Transfer*, **49**(3-4), pp. 658-670.
- [20] Shao, L., Han, J.T., and Su, G.P., et al, 2007, "Condensation Heat Transfer of R-134a in Horizontal Straight and Helically Coiled Tube-in-tube Heat Exchangers," *Journal of Hydrodynamics, Ser. B*, **19**(6), pp. 677-682.
- [21] Guo, L.J., 1989, "Dynamic Characteristics of Vapor/Gas-Liquid Two Phase Flow in Horizontal Helically-coiled Tubes," Ph.D. thesis, Xi'an Jiaotong University, Xi'an, China.
- [22] Jensen, M. K., 1980, "Boiling Heat Transfer and Critical Heat Flux in Helical Coils," Ph.D. thesis, Iowa State University of Science and Technology, USA.
- [23] Jensen, M.K., and Bergles A.E., 1982, "Critical Heat Flux in Helical Coils with a Circumferential Heat Flux Tilt toward the Outside Surface," *International Journal of Heat and Mass Transfer*, **25**(9), pp.1383-1395.
- [24] Styrikovich, M.A., Polonsky, V.S., and Reshetov, V.V., 1984, "Experimental Investigation of the Critical Heat Flux and Post-dryout Temperature Regime of Helical Coils," *International Journal of Heat and Mass Transfer*, **27**(8), pp.1245-1250.
- [25] Jayanti, S., and Berthoud, G., 1990, "High-quality Dryout in Helical Coils," *Nuclear Engineering and Design*, **122**(1-3), pp.105-118.
- [26] Ma, W.M., Zhang, M.Y., and Chen, X.J., 1995, "High-quality Critical Heat Flux in Horizontally Coiled Tubes," *Journal of Thermal Science*, **4**(3), pp.205-211.
- [27] Zhang, W.B., Zhao, L., and Chen, X.J., et al, 2009, "Investigation of Boiling Heat Transfer Deterioration of Steam/Liquid Two-Phase Flow in a Vertical Helically Coiled Tube," *Journal of Engineering Thermophysics*, **30**(10), pp.1673-1676.
- [28] Moffat, R.J., 1988, "Describing the Uncertainties in Experimental results," *Experimental Thermal and Fluid Science*, **1**(1), pp. 3-17.
- [29] Grocheveld, D.C., and Delorme, G.G.J., 1976, "Prediction of Thermal Non-Equilibrium in the Post Dry-out Regime," *Nuclear Engineering and Design*, **36**(1), pp. 17-26.
- [30] Hewitt, G.F., and Jayanti, S., 1992, "Prediction of Film Inversion in Two-phase Flow in Coiled Tubes," *Journal of Fluid Mechanics*, **236**(3), pp.497-511.